Toxicology Mechanisms and Methods

ISSN: (Print) (Online) Journal homepage: https://www.tandfonline.com/loi/itxm20

Analysis of cytotoxicity and genotoxicity in a short-term dependent manner induced by a new titanium dioxide nanoparticle in murine fibroblast cells

Matheus Pedrino, Patrícia Brassolatti, Ana Carolina Maragno Fattori, Jaqueline Bianchi, Joice Margareth de Almeida Rodolpho, Krissia Franco de Godoy, Marcelo Assis, Elson Longo, Karina Nogueira Zambone Pinto Rossi, Carlos Speglich & Fernanda de Freitas Anibal

To cite this article: Matheus Pedrino, Patrícia Brassolatti, Ana Carolina Maragno Fattori, Jaqueline Bianchi, Joice Margareth de Almeida Rodolpho, Krissia Franco de Godoy, Marcelo Assis, Elson Longo, Karina Nogueira Zambone Pinto Rossi, Carlos Speglich & Fernanda de Freitas Anibal (2021): Analysis of cytotoxicity and genotoxicity in a short-term dependent manner induced by a new titanium dioxide nanoparticle in murine fibroblast cells, Toxicology Mechanisms and Methods, DOI: 10.1080/15376516.2021.1994075

To link to this article: https://doi.org/10.1080/15376516.2021.1994075

TOXICOLOGY MECHANISMS AND METHODS
https://doi.org/10.1080/15376516.2021.1994075

Taylor & Francis
Taylor & Francis Group

RESEARCH ARTICLE

Analysis of cytotoxicity and genotoxicity in a short-term dependent manner induced by a new titanium dioxide nanoparticle in murine fibroblast cells

Matheus Pedrino[a], Patrícia Brassolatti[a], Ana Carolina Maragno Fattori[a], Jaqueline Bianchi[a], Joice Margareth de Almeida Rodolpho[a], Krissia Franco de Godoy[a], Marcelo Assis[b], Elson Longo[b], Karina Nogueira Zambone Pinto Rossi[a], Carlos Speglich[c] and Fernanda de Freitas Anibal[a]

[a]Morphology and Pathology Department, Federal University of São Carlos, São Carlos, Brazil; [b]Center of Development of Functional Materials (CDMF), Federal University of São Carlos, São Carlos, Brazil; [c]Leopoldo Américo Miguez Mello Research Center (CENPES), Rio de Janeiro, Brazil

ABSTRACT

The extensive use of titanium dioxide nanoparticles (TiO_2 NPs) in cosmetics, food, personal care products, and industries brought concerns about their possible harmful effects. Nowadays it has become important to assess TiO_2 NPs toxic effects as a way to understand their primary risks. In the cellular environment, after cell uptake, TiO_2 NPs were described to induce reactive oxygen species (ROS) production, unbalance oxidative state, and activate apoptosis in several cell lines. Therefore, we aimed to evaluate the cytotoxicity and genotoxicity of a new TiO_2 NP surface-functionalized with sodium carboxylic ligands in a murine fibroblast cell line (LA-9). TEM and DLS analyses were performed to define nanoparticle physicochemical characteristics. We evaluated the metabolic activity and LDH released after 24 h exposition to determine cytotoxic effects. Also, we evaluated DNA damage, intracellular reactive oxygen species (ROS) production, and apoptosis induction after 24 h exposure. The TiO_2 NP impaired the cell membrane integrity at 1000 μg/mL, induced intracellular ROS production and late apoptosis at 24 h. The genotoxic effects were observed at all conditions tested at 24 h. Indeed, in fibroblasts exposed at 100 μg/mL was observed early apoptosis cells. The intracellular ROS content was increased in a dose-dependent manner. Thus, short-term exposure to TiO_2 NP promoted cytotoxicity, genotoxicity and activated apoptosis pathways based on the potential role of oxygen species in the fibroblasts cell line.

ARTICLE HISTORY
Received 27 July 2021
Revised 4 September 2021
Accepted 5 October 2021

KEYWORDS
Nanomaterials; titanium dioxide nanoparticle; cytotoxicity; genotoxicity; oxidative stress; apoptosis

Introduction

Nanotechnology is a general term used for the techniques, materials, and devices developed in nanoscale, nowadays representing one of the most promising technologies for the industry. Thereby, nanotechnology grows exponentially and comprehends different fields of human knowledge (Shi et al. 2013; Vance et al. 2015; Bayda et al. 2019) being nanoparticles its most important products. Nanoparticles have dimensions equal to or smaller than 100 nm, and consequently increased surface area per unit mass, which enables to gather unique properties, such as thermal behavior, increased strength, solubility, conductivity, optical properties, and catalytic activity, contemplating a broad of applications at industrial and biomedical areas (Banfield and Zhang 2001; Kamat 2002; Nel et al. 2006; Hulla et al. 2015). For example, nanomaterials can be explored by the petrochemical industry (Khalil et al. 2017), food industry (He and Hwang 2016), and as part of materials composition in the civil industry (Azam and Akhtar 2018). Moreover, nanomaterials offer a great applicability platform due to the chemical and biological reactivity that is associated with reduced nanoparticle size (Auffan et al. 2009).

Among the nano-engineered materials, titanium dioxide nanoparticles (TiO_2 NPs) are included in the top five most applied nanomaterials in consumer products (Shi et al. 2013; Vance et al. 2015) for example in creams, cosmetics, and toothpaste (Parkin and Palgrave 2005; Samat et al. 2016) due to brightness and opacity. Also, TiO_2 NPs have been included as additives in types of cement, self-cleaning products, glasses, paints, water purification systems, and anti-fog coatings (Weir et al. 2012). TiO_2 NPs are known to be composed of crystalline mineral forms: (i) anatase, (ii) brookite, or (iii) rutile (Allen 2016; Pandey and Prajapati 2018) which are explored by industries due to photocatalytic potential. However, widespread use of TiO_2 NPs indicates an unintentional exposition risk that must be monitored by toxicological approaches.

According to IARC (International Agency for Research on Cancer), TiO_2 NPs and their derivatives are included in Group 2B classification as the agent possibly carcinogenic to humans. Also, *in vitro* and *in vivo* studies demonstrated that TiO_2 NPs trigger cellular responses like inflammation

CONTACT Fernanda de Freitas Anibal ffanibal@ufscar.br, feranibal@yahoo.com Morphology and Pathology Department, Federal University of São Carlos, São Carlos, 13565-905 Brazil.

(Giovanni et al. 2015), oxidative stress (Hu et al. 2015), and apoptosis (Márquez-Ramírez et al. 2012) which can contribute to toxicity. Unlike, some studies indicated that TiO_2 NPs are harmless and non-cytotoxic nanomaterials (Kocbek et al. 2010; Rosłon et al. 2019; Líšková et al. 2020). This way it remains unclear which cellular response triggered by TiO_2 NPs is responsible for toxicity in a general perspective and which modulates its safety use. However, anatase TiO_2 NPs have higher toxic effects compared with rutile crystalline form (Clemente et al. 2015) which are associated with photocatalytic potential. Hence, *in vitro* studies are interested in understanding oxidative stress cascades initiated by TiO_2 NPs exposure and address a potential contribution to toxicity (Song et al. 2016).

In a cellular environment, after cell uptake, TiO_2 NPs are described to induce reactive oxygen species (ROS) production, unbalance oxidative state, and activate apoptosis in several cell lines. In a human bronchial epithelial cell (BEAS-B), TiO_2 NPs induced ROS formation, decreased antioxidant enzymes levels and activated apoptosis (Park et al. 2008). TiO_2 NPs also increased ROS levels and promoted genotoxic effects in HaCat keratinocytes (Jaeger et al. 2012) and human epidermal cells (A431) (Shukla et al. 2011). ROS formation by TiO_2 NPs exposure also was associated with cell cycle dysfunction followed by DNA damage (Kansara et al. 2015). In fibroblasts, TiO_2 NPs modulated ROS production, lactate dehydrogenase release, and affected cell viability (Jin et al. 2008). Then, it is demonstrated that TiO_2 NPs have a toxicity profile based on the potential role of oxidative stress and that was explored further to understand its main cellular effects.

In general, the mechanisms of toxicity related to TiO_2 NPs are described to regulate ROS production and affect essential cellular processes and components. Genome-wide analysis (RNA-Seq) showed that TiO_2 NPs promote endoplasmic reticulum stress which can be linked with ROS generation and interfere with plasma glucose metabolism in mice (Hu et al. 2019). Also, mitochondria damage, lysosomes rupture, and other organelles injuries are associated with TiO_2 NPs exposure leading to toxic phenotypes (Liu and Tang 2020). Moreover, studies tried to investigate the following effects upon ROS production that contributed to toxicity in living organisms. Oxidative stress modulated by TiO_2 NPs can increase lipid peroxidation, cell membrane damage, cause indirect or direct genotoxic effects, and trigger apoptosis (Hou et al. 2019). The last can be promoted by plenty of signaling pathways linked with organelles and DNA damage. Hence, nanotoxicology is seeking *in vitro* approaches to understand the most pronounced toxic effect of TiO_2 NPs in a way to apply its use safely.

Thus, we aimed to evaluate the cytotoxicity and genotoxicity of a new titanium dioxide nanoparticle composed of anatase and surface modified with sodium carboxylate ligands. Indeed, we explored intracellular ROS production, and cell death promotion to establish its mechanism of toxicity. The nanoparticle was previously synthesized to own a better dispersal in comparison with other nanomaterials available in the market. Besides, this nanoparticle has a great destination for PETROBRAS, that seeks to apply this TiO_2 NP in the oil extraction process (Khalil et al. 2017). Aligned with PETROBRAS, our work was the first step to study nano toxicological aspects of this new nanoparticle, based on the fibroblast cell line. We expected that TiO_2 NP would present low harmful effects on cell culture models based on its surface modification and physicochemical properties.

Materials and methods

Nanoparticle dispersion and characterization (DLS/TEM)

Titanium dioxide nanoparticle was obtained from Leopoldo Américo Miguez Mello Research Center (CENPES) located in Rio de Janeiro, Brazil. The nanoparticle is made of titanium dioxide nucleus composed only of anatase crystalline structure and surface-modified with carboxylic sodium ligands (COOH–Na+). Just after synthesis, TiO_2NP was characterized by Dynamic Light Scattering (DLS) and Transmission Electron Microscopy (TEM).

To improve our comprehension about nano biological interactions, TiO_2 NP suspensions (1000, 100, and 10 μg/mL) were characterized in DMEM (Dulbecco's Modified Eagle's Medium – Sigma-Aldrich) without phenol and supplemented with 10% fetal bovine serum (FBS). After mixing and stirring, each suspension was analyzed by DLS to determine the mean hydrodynamic size (Zav). Zeta-potential (mV) was determined with suspensions prepared in ultrapure water. DLS analysis was carried out in a Zetasizer Nano (ZS90) considering three independent intensity and volume measurements. All the data were merged for size and volume distribution.

Transmission electron microscopy (TEM) was performed in a Jem-2100 LaB6 (Jeol) microscope operating at 200 kV. The samples were prepared by depositing small drops of the TiO_2 NP dispersions in DMEM directly onto holed carbon-coated Cu grids.

Cell culture

Murine-derived fibroblasts cell line (LA-9) was purchased from Rio de Janeiro Cell Bank (BCRJ-Brazil). The LA-9 cell line was cultured in DMEM supplemented with 10% FBS, 10 mM sodium pyruvate, 1.5 g/L sodium bicarbonate, and 1% streptomycin/penicillin. Fibroblasts were grown and maintained in T-75 flasks (KASVI) at 37 °C in a 5% CO_2 air incubator (Thermo-Fisher) before *in vitro* analysis.

Cytotoxicity assay (MTT)

The colorimetric assay with tetrazolium salt MTT (3-(4,5-Dimethylthiazol-2-yl)-2,5- diphenyl tetrazolium bromide) was useful to access the metabolic activity of fibroblasts after TiO_2NP exposure. After being exposed by treatments, only viable cells are capable to reduce MTT salt into formazan crystals which are dissolved, promoting a yellow-purple color change detectable by a spectrophotometer and correlated with cell viability (Mosmann 1983). For MTT assay, 3×10^4 fibroblasts (LA-9) were

seeded and grown in 96-well plates (KASVI) for 24 h (6-wells per condition) in an incubator at 37 °C/5% CO_2. After cell adhesion, the medium was replaced with TiO_2 NP treatments (1000, 100, and 10 μg/mL) for 24 h. At the end of exposition time, the TiO_2 NP treatments were removed, each well was washed twice with sterile 1x phosphate buffer saline (PBS) and added 200 μL 0.5 mg/mL MTT solution (Sigma-Aldrich).

The cells with MTT were incubated at 37 °C/5% CO_2 for at least 3 h and the formazan crystals were dissolved with 100 μL DMSO (Synth). Absorbance was measured at 570 nm in a reader plate MultiSkan Go (Thermo-Fisher) and cell viability percentage was calculated in comparison with the control group (without TiO_2 NP treatment) according to the Equation (1) . We highlight here that based on MTT assay results, 24 h time point of exposure was selected to perform all further analysis.

$$\text{Cell viability } (\%) = \frac{\text{Absorbance treatment} \times 100}{\text{Absorbance negative control}} \quad (1)$$

Cell damage assay (LDH)

TiO_2 NP effects on cell membrane integrity were evaluated by lactate dehydrogenase release according to colorimetric CyQuant LDH Cytotoxicity Assay Kit (Invitrogen). For the LDH assay, 1×10^4 cells/well were seeded and grown in 96-well plates (KASVI) for 24 h (6-wells per condition) in an incubator at 37 °C/5% CO_2. Then, TiO_2 NP treatments (1000, 100, and 10 μg/mL) were added at each well, and fibroblasts were incubated for 24 h at 37 °C/5% CO_2. Absorbance was measured at 490 nm in a reader plate MultiSkan Go (Thermo-Fisher) and cell damage percentage was calculated in comparison with the control group (without TiO_2 NP treatment).

Cell morphology by optical microscopy

The fibroblasts (LA-9) were visualized after TiO_2 NP exposition (1000, 100, and 10 μg/mL) for 24 h, and images were captured using an Axiovert 40 CFL (Zeiss) with a 10× objective lens. A camera model LOD-3000 (BioFocus) was coupled to improve the image acquisition. Images were analyzed using the software Future WinJoe v.2 (Schindelin et al. 2012).

Intracellular ROS measurement

Intracellular ROS content in fibroblasts exposed to TiO_2 NP was measured using the fluorescence probe 2,7-dichlorofluorescein diacetate activation (DCFH-DA) (Sigma-Aldrich). Briefly, fibroblasts were seeded in a 96-well black assay plate at 1×10^4 cells/mL and incubated with TiO_2 NP (1000, 100, and 10 μg/mL) for 24 h. Serum starved medium was used as negative control (C^-). After 24 h, fibroblasts were incubated with DCFH-DA for 30 min and each well was washed with 1x PBS . Fluorescence intensity was determined using a SpectraMAX i3® plate spectrophotometer (Molecular Devices) with excitation and emission wavelengths at 485 and 530 nm respectively.

Genotoxicity assay (comet)

TiO_2 NP genotoxic effects were accessed by Comet Assay, a standard approach in nanotoxicology studies that can help to identify DNA breaks from different origins (oxidative damage, abasic sites, etc). The genotoxicity assay was performed in a fibroblast cell line (LA-9) with two independent replicates in at least two biological samples per group tested. For Comet assay, 2.5×10^5 cells/well were seeded and grown in 24-well plates (KASVI) for 24 h (3-wells per condition) at 37 °C in a 5% CO_2/air incubator. After cell attachment, the medium was removed and cells were incubated with TiO_2 NP treatments (100, 10, and 1 μg/mL) for 24 h. We did not use experimental conditions > 100 μg/mL TiO_2 NP due to possible nanoparticle interference with Comet Assay (Guadagnini et al. 2015). Also, the assay contained a control positive group (C^+) with cells exposed to 70 μM methyl methanesulfonate (MMS) solution (Sigma-Aldrich) and a control negative group (C^-) with cells unexposed to the nanoparticle. At the end of time exposure, all the treatments were removed from the plate, cells were washed twice with 1× PBS and detached with 0.25% trypsin/EDTA (LGC Biotechnology) at 37 °C for 5 min. Cells in suspension were collected in 1.5 mL microtubes after centrifugation at 219 × *g* for 5 min.

Before electrophoresis, cell viability was determined for all the tested groups by 0.4% Blue Trypan staining. Only groups with cell viability > 80% were used in the next steps. Then, 20 μL cell suspensions were mixed with 120 μL agarose LMP (Low Melting Point – Invitrogen), dripping at a slide pre-coated with agarose1.5% and covered with 24 × 50 mm coverslips. Slides (3 per group) were allowed to solidify at 4 °C for 20 min, the coverslips were removed and the slides were incubated in a fresh cold lysis solution (2.5 M NaCl, 100 mM EDTA, 10 mM Tris, 10% DMSO , 1% Triton X-100 with pH > 10) for 1.5 h in the dark. After lysis, slides were transferred to a cold alkaline electrophoresis solution (200 mM EDTA tritriplex, 10 N NaOH, pH > 13) for 20 min to enable the denaturation of DNA. Electrophoresis was conducted in an electric field with 28 V (0.8 V/cm) and approximately 300 mA for 20 min. After electrophoresis, slides were washed three times with a neutralization solution (0.3 M Tris, pH = 7.5) and then were thawed/fixed within ethanol 100% for 10 min. The staining was performed with 0.03% GelRed solution (Biotium, Uniscience), the comets were then visualized and counted (at least 100 per slide) in a fluorescence microscope (Olympus) connected to a camera with an excitation filter of 510–560 nm and a barrier filter of 590 nm, at a magnification of 400×. DNA damage was visually evaluated according to the tail size and classified in class 0: without visual damage; 1: small damage; 2: average damage; 3: large damage (Kobayashi et al. 1995). Score DNA damage was calculated for all treatment groups based on Equation (2).

$$\text{Score DNA damage} = ([0 \times \text{class } 0] + [1 \times \text{class } 1] + [2 \times \text{class } 2] + [3 \times \text{class } 3]) \quad (2)$$

Apoptosis induction by nanoparticle

Early and late apoptosis were assessed by flow cytometry using Annexin V and 7-amino-actinomycin D (7-AAD) markers

according to BD Biosciences detection kit instructions. Fibroblasts were seeded in a 24-well assay plate at 1×10^5 cells/well and cultured for 24 h. Then, cells were incubated with TiO_2 NP (1000, 100, and 10 μg/mL) for 24 h. After the exposure period, cells were washed with 1x PBS buffer, and the PE Annexin V and 7-AAD antibodies were added to each well diluted in Binding Buffer. The plate was incubated at 4 °C for 15 min for antibody reaction recognition. The data acquisition was performed in an Accuri ™ C6 BD Biosciences flow cytometer (gate 10.000 events) and all data were analyzed using the software FlowJo 10.7.1 (BD Biosciences).

In addition, apoptosis induction was evaluated in fibroblasts stained with acridine orange (LA) and propidium iodide (PI) after nanoparticle exposure. Fibroblasts were cultured in a 96-well assay plate at 1×10^4 cells/well and exposed to TiO_2 NP (1000, 100, and 10 μg/mL) for 24 h. Then, the supernatant of the cell was removed and 30 μL 0.1% LA/PI (1:1) solution was added at each well and incubated for 15 min. Then, image acquisition was performed in an automated high-resolution epifluorescence microscopy system ImageXpress Micro (Molecular devices) using a 40× objective lens and equipped with FITC and Texas Red filters to obtain image overlays.

Statistical analysis

All data represent mean ± standard error of the mean (SEM) from at least two independent experiments. Statistical analysis was performed using Graph Pad Prism (v.7, San Francisco, CA, USA) by One-way ANOVA (One-way Analysis of Variance) with Bonferroni post hoc correction. Significance level was adopted as 5% with $^*p < 0.05$, $^{**}p < 0.01$ and, $^{***}p < 0.001$.

Results

Nanoparticle characterization

TiO_2 NP primary physicochemical characteristics were determined by TEM and DLS analysis. It is important to highlight that this nanoparticle is not a commercial product and was developed for application-related purposes within the petrochemical industry in Brazil. According to Figure 1(A), TiO_2 NP at 10 μg/mL showed good dispersibility with an average size of 12.3 nm in the culture medium. Otherwise, TiO_2 NP at 100 μg/mL and 1000 μg/mL (Figure 1(B,C)) form larger aggregates, with an average particle size of 13.9 and 14.3 nm respectively. In this way, the increase in the concentration of TiO_2 NP particles in the culture medium causes a greater aggregation of the TiO_2 NP particles. In addition, it can be seen by the Fast Fourier transform (FFT) that all samples are referring to anatase, a tetragonal TiO_2 phase belonging to the spatial group *I41/amd*. This is due to the presence of the planes (101) and (100), with interplanar distances of 0.352 and 0.189 nm respectively (Horn et al. 1972). Also, we noticed that the small size of nanoparticle interfered in TEM images resolution in all concentrations analyzed (Table 1).

TiO_2 NP suspensions in DMEM supplemented with 10% FBS exhibited a hydrodynamic size of 23.7 ± 0.50,

Table 1. TiO_2 NP secondary physicochemical characterization.

[TiO_2 NP]	Zav (nm)	Zeta Potential (mV)	PdI
1000 μg/mL	87.26 ± 6.3	−22.9 ± 0.75	0.28 ± 0.01
100 μg/mL	29.81 ± 1.044	−21.7 ± 5.2	0.43 ± 0.03
10 μg/mL	23.77 ± 0.50	−10.1 ± 4.9	0.47 ± 0.01

All data were obtained in a Zetasizer Nano and represent the means ± SEM. Zav: hydrodynamic size; PdI: polydispersity index. The nanoparticle zeta-potential was determined in ultrapure water suspension. PdI represents the distribution and variability among size measurements.

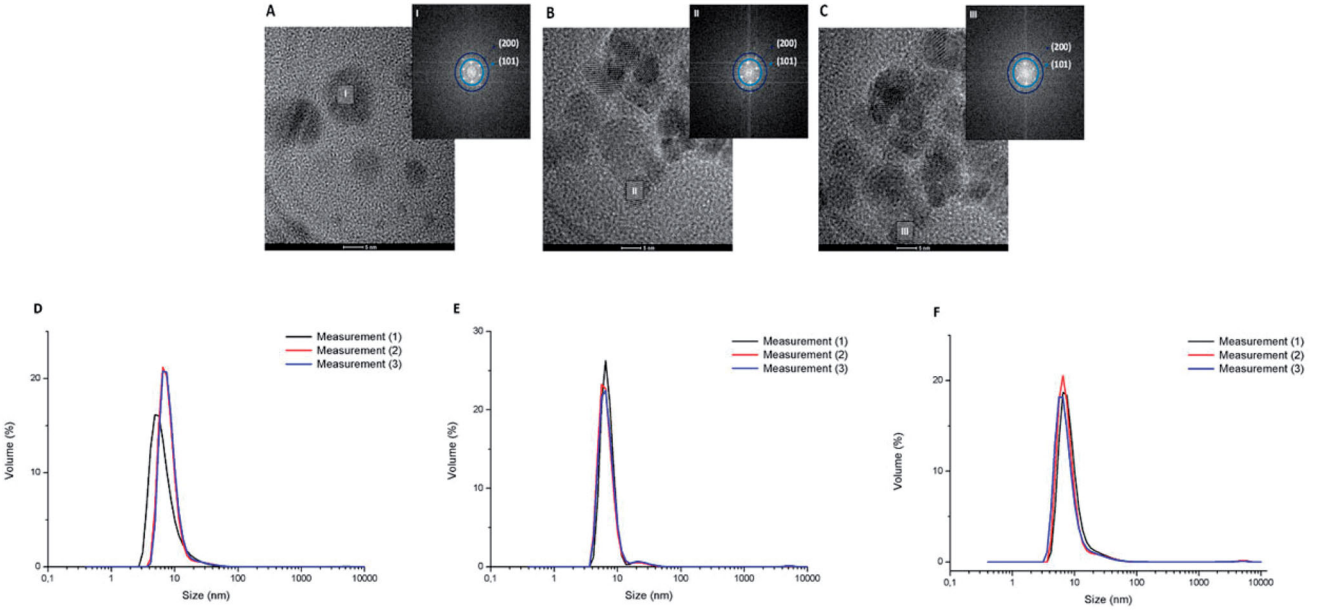

Figure 1. TiO_2NP transmission electron microscopy (TEM) images at 10 μg/mL (A), 100 μg/mL (B), and 1000 μg/mL (C). All images showed the tetragonal phase which characterizes the anatase crystalline form of TiO_2 NP with its measurements performed by the fast Fourier transform (FFT). Dynamic light scattering (DLS) plot showing TiO_2 NP size distribution at 10 μg/mL (D), 100 μg/mL (E), and 1000 μg/mL (F). DLS data were obtained with TiO_2NP dispersed on DMEM supplemented with 10% FBS.

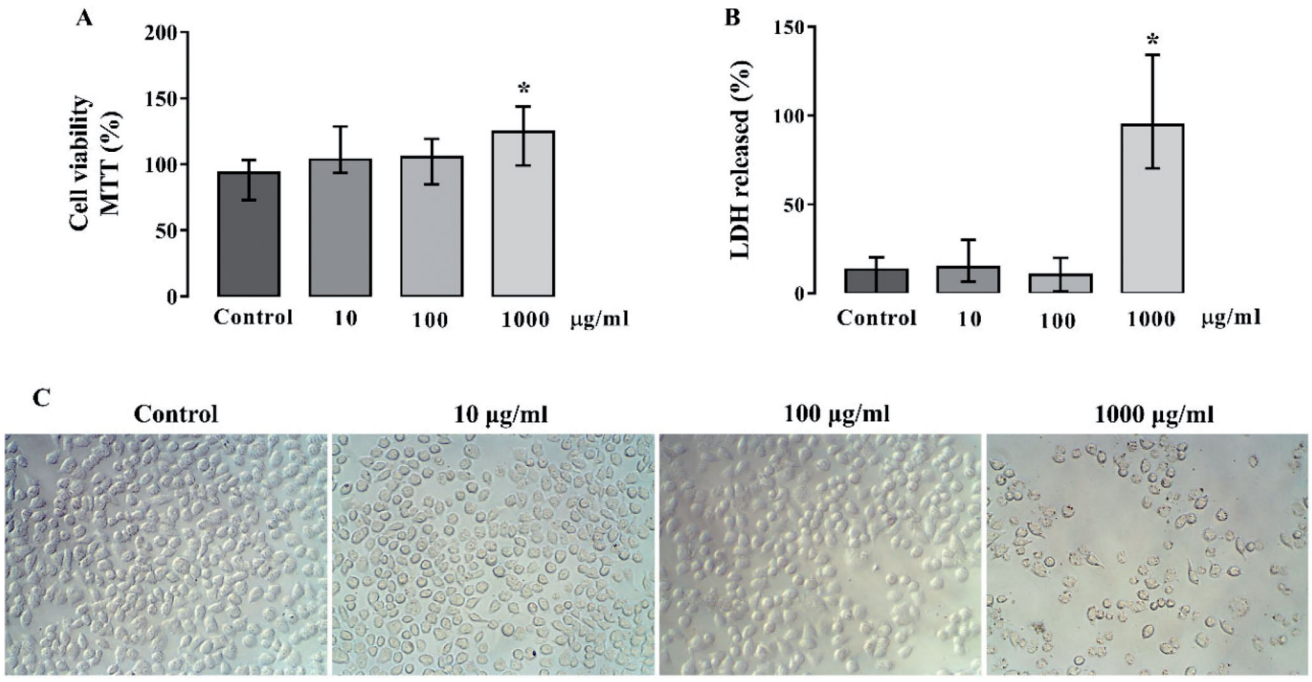

Figure 2. TiO_2 NP cytotoxic effects. MTT assay results (A) and LDH released activity (B) in fibroblasts (LA-9) after TiO_2 NP exposure for 24 h; (C) optical microscopy images visualizing fibroblast morphology after TiO_2 NP exposure. (*) vs. control; $^*p < 0.5$.

29.8 ± 1.044, and 87.3 ± 6.3 respectively for 10, 100, and 1000 µg/mL concentrations by DLS (Figure 1(D–F)). Nanoparticle polydispersity index (PdI) was 0.47 ± 0.01, 0.43 ± 0.03 and 0.28 ± 0.01 respectively for 10, 100 and 1000 µg/mL TiO_2 NP concentrations. At 1000 µg/mL, TiO_2 NP showed a higher increase in hydrodynamic size and achieved the highest zeta-potential value (–22.9 ± 0.75) among the concentrations analyzed.

Cytotoxic and cell membrane damage effects

The MTT assay was performed to evaluate the metabolic activity of fibroblasts exposed to the nanoparticle for 24 h which might be an indicator of cytotoxicity. The TiO_2 NP did not show cytotoxic effects (Figure 2(A)) in any concentrations tested (1000, 100, and 10 µg/mL) to fibroblast cells (LA-9) over time compared with the control group. Additionally, the release of lactate dehydrogenase was evaluated after nanoparticle exposure to determine the level of cell membrane disruption in fibroblasts, which might be associated with necrosis cell damage and apoptosis. TiO_2 NP induced the highest level of LDH release in fibroblasts at 1000 µg/mL compared with the control group after 24 h (Figure 2(B)). At 100 and 10 µg/mL of TiO_2 NP, the release of LDH was equal or lower compared with the control group.

Intracellular ROS measurement

We evaluated the reactive oxygen species production in fibroblasts after TiO_2 NP exposure at 24 h using the fluorescence probe DCFH-DA. There was a significant increase in ROS generation in fibroblasts exposed at 100 and 1000 µg/mL TiO_2 NP compared with the control group (Figure 3(A)) according to quantitative analysis of fluorescence. The highest ROS levels were detected in fibroblasts exposed to 1000 µg/mL although we cannot notice this change by qualitative analysis (Figure 3(B)).

Genotoxic effects

DNA damage potential associated with TiO_2 NP was evaluated using the Comet assay in alkaline conditions which might detect primary DNA lesions as alkali-labile sites, abasic sites, single and double-strands break, crosslinks, and incomplete repair sites. The assay showed (Figure 4) genotoxic effects in fibroblasts exposed to 100, 10, and 1 µg/mL of TiO_2 NP at 24 h compared with unexposed cells (control group). The damage was dose-dependent on this period and achieved the highest score at 100 µg/mL compared with other treatments. Moreover, all groups analyzed by Comet Assay had > 90% of cell viability assessed by Blue Trypan staining prior to electrophoresis.

Apoptosis induction upon nanoparticle exposure

Flow cytometry was used with associated markers Annexin V (PE) and 7-AAD to discriminate between cells undergoing early or late apoptosis respectively in fibroblasts exposed to TiO_2 NP (1000, 100, and 10 µg/mL) at 24 h. All the TiO_2 NP concentrations were capable of inducing early apoptosis in fibroblasts compared with the control group (Figure 5(A,C)). Fibroblasts exposed to 100 and 1000 µg/mL TiO_2 NP showed the highest level of early and late apoptosis induction respectively. The same profile is represented in histograms of fibroblast cells (LA-9) after 24 h of apoptosis induced by the nanoparticle in a range of concentrations.

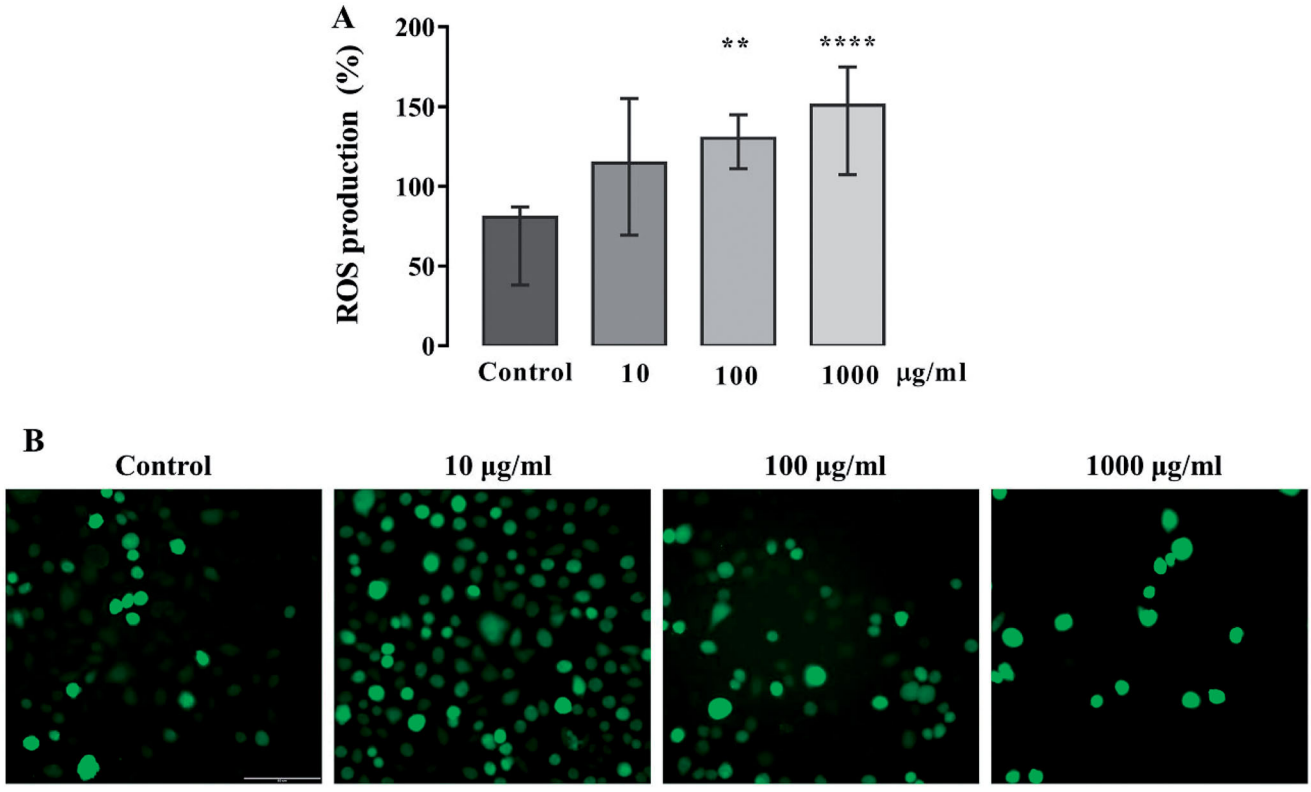

Figure 3. Intracellular ROS production (A) and fluorescence ROS intensity images (B) visualized in fibroblasts (LA-9) exposed to TiO_2NP after 24 h. Cells were exposed to 10, 100 and 1000 µg/ml of TiO_2 NP and control (cells + medium). The results show the comparison of the concentrations evaluated in parallel to the control. (*) vs. control; $^{**}p < 0.01$; $^{****}p < 0.0001$.

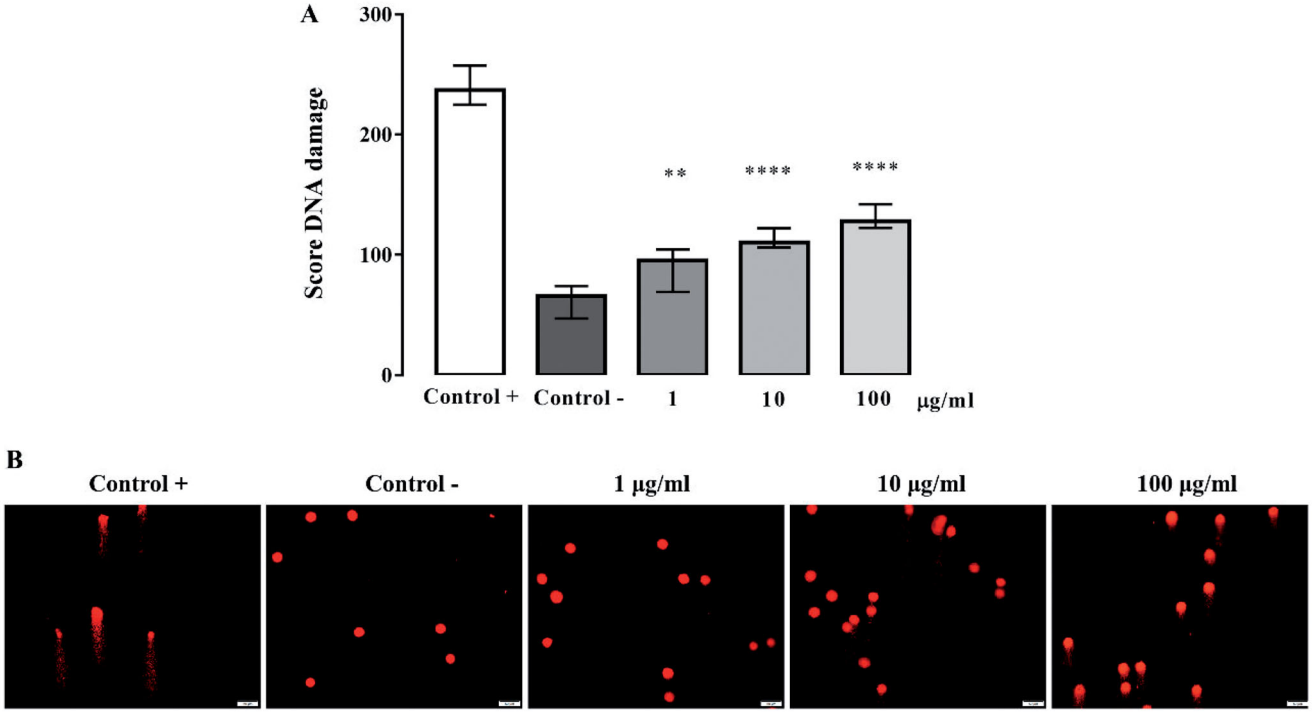

Figure 4. DNA damage induced by TiO_2 NP after exposure to fibroblasts (LA-9) for 24 h. Control (–) represents cells unexposed to nanoparticle; control (+) represents cells exposed to MMS 70 uM solution. Results represent the average of the scores ± SEM per group. Score: (percentage of cells in class 0 × 0) + (percentage of cells in class 1 × 1) + (percentage of cells in class 2 × 2) + (percentage of cells in class 3 × 3). The statistical analysis was performed comparing the control group with TiO_2 NP treatments by one-away ANOVA (Bonferroni *post-hoc* correction); $^{**}p < 0.01$ and $^{****}p < 0.0001$.

Figure 5 (B) shows the high-resolution epifluorescence microscopy images made with overlapping from the FITC and Texas Red filters of fibroblasts exposed to TiO_2 NP for 24 h and stained with acridine orange, which emits green fluorescence and marks living and dead cells, while propidium iodide marks dead cells in which the reddish cytoplasm

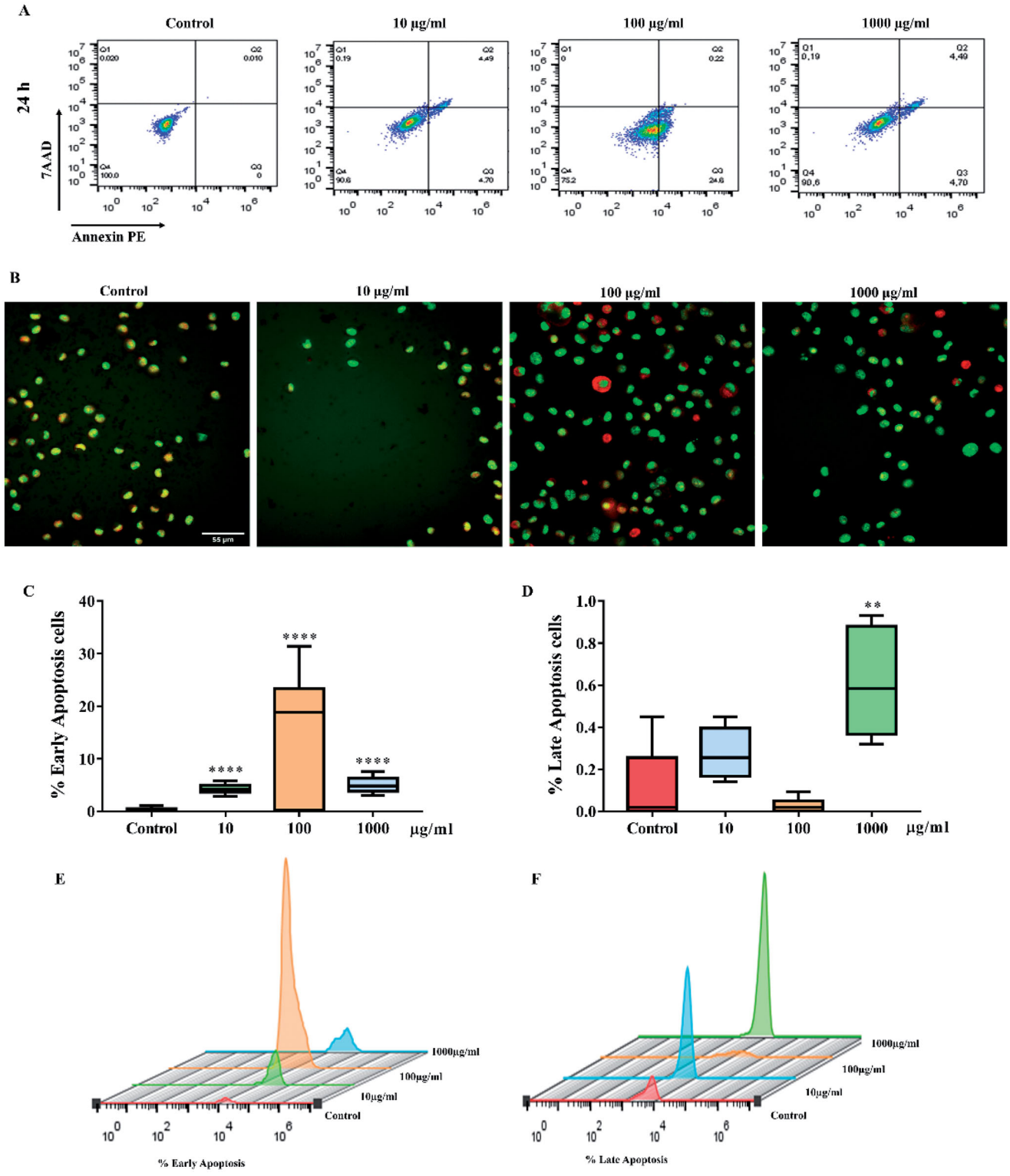

Figure 5. Apoptosis induction in fibroblasts (LA-9) after TiO_2 NP exposition for 24 h. (A) Histograms of each analyzed TiO_2 NP condition (10; 100; and 1000 µg/ml) and control (cells + medium). (B) Demonstrative analysis of fibroblasts (LA-9) stained with acridine orange (AO) and propidium iodide (IP) fluorophores 24 h after exposure to different concentrations of TiO_2 NP showing cell death through overlapping images obtained using an automated high-resolution epifluorescence microscopy system. (C and D) Percentage of early apoptotic and late apoptotic cells. (E and F) Each peak of fluorescence emission. (*) vs. control; $^{**}p < 0.01$; $^{****}p < 0.0001$.

and nucleus indicates initial apoptosis and necrosis or late apoptosis respectively. In parallel with flow cytometry results, imaged fibroblasts LA-9 exposed to 100 and 1000 µg/mL TiO_2 NP had an increasing stain for dead cells observed with reddish cytoplasm and nucleus characteristics.

Discussion

According to the wide array of TiO_2 NPs applications in different industry sectors, we evaluated the cytotoxic and genotoxic potential of a new titanium dioxide nanoparticle using

a fibroblast cells culture (LA-9). Additionally, we investigated oxidative stress unbalance effects and apoptosis induction in the same cell line. This work is the first report seeking to comprehend toxicological aspects and the biological behavior of this new nanoparticle using an *in vitro* model. Our approach to studying this nanoparticle was based on the interest of the PETROBRAS industry that will apply TiO_2 NP in the petroleum extraction process. Thereby, the aim was to understand nanoparticle primer effects upon cytotoxicity until its interference on the intracellular environment triggered by cell uptake followed by ROS production, DNA damage, and apoptosis.

First, we aimed to determine the TiO_2 NP physicochemical characteristics in a biological environment simulating cell culture conditions. We observed that TiO_2 NP dispersed on DMEM medium was not stable based on PdI values, which probably increased hydrodynamic size. In general, nanoparticles have a reactive surface capable of adsorbing biomolecules (proteins, lipids, and polysaccharides) and create a surface layer known as protein corona (PC) (Liu et al. 2020). Then, the aggregation and agglomeration state of nanoparticles might be a cause of their increased size and instability in cell culture conditions. Moreover, PC formation in nanoparticles is well-known as a dynamic process (Cedervall et al. 2007) described by 'the Vroman effect' (Vroman 1962) commonly dependent on other nanoparticles characteristics such as size, composition, shape, time, the temperature of incubation, etc. An example of PC formation was yet observed in another TiO_2 NP that had an increased hydrodynamic size range (30–500 nm) in FBS dispersion (Gunnarsson et al. 2018), signaling a common effect on this knowledge area. Beyond that, PC is largely described as a variability cause and responsible for interfering in nano toxicological analyses (Liu et al. 2020), being a difficult task to determine PC composition due to the complex interaction between cell and biological components. Also, according to zeta-potential, we suggested that nanoparticles might have a negative surface charge, aligned with sodium carboxylic functionalization, which interferes with cell uptake pathways, toxicity and modify the environment pH consequently affecting dispersion stability. About surface charge, it is described that those nanoparticles positively charged interact easier with the cellular membrane, which increases its uptake rate and promotes higher cytotoxicity (Nel et al. 2009; Arvizo et al. 2010). Taken together, size and charge interpose nano biological interactions, cell uptake (Rivera-gil et al. 2013), and could play a role in TiO_2 NP cytotoxicity and genotoxicity.

About TiO_2 NP cytotoxicity, Hamzeh and collaborators (Hamzeh and Sunahara 2013) showed that a TiO_2 NP (anatase) at 10 and 100 mg/L decreased L929 fibroblast cell viability in culture after 24 and 48 h. Likewise, TiO_2 NP cytotoxicity was described as dose and time-dependent by (Jin et al. 2008) that observed a decrease (37%) in L929 fibroblast's cell viability after exposure to TiO_2 NP ($3 - 600$ μg/ml) for 48 h. Also, it was indicated that 50 and 100 μg/ml TiO_2 NP in 3T3 fibroblasts reduced cell viability in a dose and time-dependent manner (Tripathi et al. 2018). Our results related to TiO_2 NP cytotoxicity (MTT assay) do not corroborate with those previous findings as we aimed to evaluate nanoparticle effects at short-term exposure (24 h) being TiO_2 NP not cytotoxic to fibroblasts in any dose at this period. Even without direct effects on mitochondrial metabolism, morphological changes were observed in fibroblasts exposed to TiO_2 NP compared with the negative control group, which suggests effects on the cell membrane unexplored.

Inside the cell, a nanoparticle may cause multiple types of damage as exemplified by oxidative stress arising from metal ions released (Wu et al. 2010; Bannunah et al. 2014; Klingberg et al. 2015). Consequently, TiO_2 NP is supposed to affect cells in two distinct ways: cell membrane damage (1) or genetic material impairment (2). When the last occurs, nanoparticles trigger a genotoxicity process that can be initiated by a direct disturbance in the cell membrane by interfering with hydrophobic interactions or in the membrane permeability (Wong-Ekkabut et al. 2007). We observed higher levels of LDH released in fibroblasts cell supernatant when exposed at 1000 μg/mL TiO_2 NP indicating cell membrane injuries following high genotoxic effects at $\geq$ 100 μg/mL TiO_2 NP. Also, it is worth noting, as reported by Gholinejad and collaborators, that extracellular LDH levels and intracellular ROS production are correlated and maybe a good indicator of genotoxic effects triggered by cell membrane damage or oxidative unbalance as observed.

In general, genotoxicity is known to result from direct or indirect effectors. Here, we highlight the importance of an indirect genotoxic factor related to chronic inflammation caused by (i) immune system activation or (ii) a route of mitochondria damage that leads to increased ROS production and consequently impairs genetic material (Ali et al. 2016). The reactive oxygen species are involved in many cellular mechanisms including cell cycle regulation, proliferation and differentiation, cell self-renewal, and apoptosis (Kim et al. 2010; Gholinejad et al. 2019). In turn, cells developed defense mechanisms to maintain the intracellular oxidative balance as the tumor suppressor protein p53 that controls cell cycle arrest and allows DNA damage repair (Benchimol 2001). However, damages that cannot be repaired may lead to cell death by apoptosis.

According to this perspective, our study demonstrated that short-term exposure to TiO_2 NP led to increased ROS production and consequently high DNA damage in fibroblasts (LA-9) which could be associated with nanoparticle crystalline form and size. It is described that mineral composition modifies the genotoxic effects of nanomaterials (Chen et al. 2014), including TiO_2 anatase, a well-known crystalline structure that promotes more adverse biological effects such as cytotoxicity, inflammation, and ROS formation (Sayes et al. 2006; Falck et al. 2009). Reactive oxygen species are broadly coupled along with TiO_2 NPs exposure and pointed as one of the causes for DNA lesions (Fujishima and Zhang 2006; Linkov et al. 2008) corroborating our achievements. According to Hamzeh and collaborators, three types of TiO_2 NP composed of anatase or mixture anatase/rutile induced DNA damage in hamster fibroblasts cells treated with 100 mg/mL. Another study found genotoxic effects of a TiO_2

NP (<25 nm) in dolphin leukocytes cells after treatments with 50 and 100 μg/mL at 24 and 48 h (Bernardeschi et al. 2010). Then, we suggested that agglomeration level, size and crystalline mineral form of TiO_2 NP induced an increasing ROS production (≥1000 μg/mL), contributing to higher TiO_2 NP genotoxicity.

Based on the oxidative unbalance and genotoxic effects that are related to cell death by apoptosis (Wang 2001), we performed flow cytometry using Annexin V and 7-AAD markers to determine apoptosis profile in fibroblasts exposed to TiO_2 NP. Late apoptotic fibroblasts ($Annexin^-/7\text{-}ADD^+$) were observed after 1000 μg/ml TiO_2 NP exposure in parallel with high LDH releasing. According to (Elmore 2007), late apoptosis is a passive process, non-controlled and triggered by energy metabolism impairment and cell membrane damage. In other words, fibroblasts exposed to the highest nanoparticle dose were identified at the late apoptosis stage probably due to cell membrane damage following DNA damage. Otherwise, early apoptotic fibroblasts ($AnnexinV^+/7\text{-}ADD^-$) were observed after 100 μg/ml TiO_2 NP exposure described in the literature as a result of DNA breaks (Gholinejad et al. 2019), and that was described by our Comet assay result. Interestingly, the early apoptosis mechanism triggered by TiO_2 NP is described as dose-dependent i.e. apoptosis states can be very dissimilar according to nanoparticle concentration, as corroborated by flow cytometry and epifluorescence images. In human neuron cells, titanium at micro and nano-scale was capable to induce apoptosis in a dose-dependent way (Stoccoro et al. 2016). Also, was observed differentiated cells marked to early or late apoptosis, including double marked cells, demonstrated a great complexity to understand the real effects of nanomaterials and that must be explored in future investigations.

Thus, we may suggest a short-term toxicity mechanism to the new TiO_2 NP observed in fibroblasts by initial increased cell damage at high concentration followed by the potential role of oxidative stress. The cell oxidative balance was probably the main factor to induce DNA damage by direct ROS action into the nucleus. Finally, apoptosis status was also modified upon nanoparticle exposure and can represent the last response of fibroblasts.

Conclusion

Our work aimed to evaluate the cytotoxicity and genotoxicity of a new titanium dioxide nanoparticle surface modified with sodium carboxylic ligands. Additionally, we tried to understand the main TiO_2 NP mechanism of toxicity using approaches to detect intracellular ROS production and apoptosis induction. At short-term exposure, TiO_2 NP caused genotoxic effects at all conditions tested and cell membrane damage at ≥1000 μg/ml. Also, TiO_2 NP was capable to induce intracellular ROS production in fibroblasts which might be related to DNA damage and apoptosis induction. We found that TiO_2 NP was capable to induce early and late apoptosis in a dose-dependent manner, being 1000 μg/ml and 100 μg/ml associated with late and early apoptosis pathways, respectively. Moreover, we highlighted the necessity to further understand TiO_2 NP cytotoxic and genotoxic effects on different cell lines after the long-term exposition and to better recognize its harmful effects. However, our findings presented here were the first step on further toxicity analysis to define the best work conditions with this new nanomaterial.

Acknowledgments

The authors acknowledge the PETROBRAS for all financial support during the work execution. M.P., A.C.M.F. and P.B. were grateful respectively to PETROBRAS Masters, PhD and post-doctoral fellowships. We thank the Post-Graduation Program of Evolutionary Genetics and Molecular Biology from UFSCar, Prof. Dr. Marcos Roberto Chiaratti (UFSCar) and Prof. Dra. Marisa Narciso Fernandes (UFSCar) for kindly providing technical assistance in Comet assay analysis, and Prof. Dr. Valtencir Zucolotto (USP) for providing all the assistance for DLS analysis. We also thank all the Nano-PETROBRAS project team members who assisted indirectly to this work. We also acknowledge Fundação de Amparo à Pesquisa do Estado de São Paulo - FAPESP (2013/07296-2), FINEP, Conselho Nacional de Desenvolvimento Científico e Tecnológico – CNPq (166281/2017-4), Financiadora de Estudos e Projetos – FINEP, and Coordenação de Aperfeiçoamento de Pessoal de Nível Superior – CAPES (001).

Disclosure statement

No potential conflict of interest was reported by the author(s).

Funding

This research was funded by Petróleo Brasileiro S.A (PETROBRAS/ N° 2017/00010-7); CENPES-RJ, Fundação de Amparo à Pesquisa do Estado de São Paulo - FAPESP (2013/07296-2), FINEP, Conselho Nacional de Desenvolvimento Científico e Tecnológico – CNPq (166281/2017-4), Financiadora de Estudos e Projetos – FINEP, and Coordenação de Aperfeiçoamento de Pessoal de Nível Superior – CAPES (001).

References

Ali A, Suhail M, Mathew S, Shah MA, Harakeh SM, Ahmad S, Kazmi Z, Alhamdan MAR, Chaudhary A, Damanhouri GA, Qadri I. 2016. Nanomaterial induced immune responses and cytotoxicity. J Nanosci Nanotechnol. 16(1):40–57.

Allen R. 2016. The cytotoxic and genotoxic potential of titanium dioxide (TiO_2) nanoparticles on human SH-SY5Y neuronal cells in vitro. Plymouth Student Scientist. 9(92):5–28.

Arvizo RR, Miranda OR, Thompson MA, Pabelick CM, Bhattacharya R, Robertson JD, Rotello VM, Prakash YS, Mukherjee P. 2010. Effect of nanoparticle surface charge at the plasma membrane and beyond. Nano Lett. 10(7):2543–2548.

Auffan M, Rose J, Bottero JY, Lowry GV, Jolivet JP, Wiesner MR. 2009. Towards a definition of inorganic nanoparticles from an environmental, health and safety perspective. Nat Nanotechnol. 4(10):634–641.

Azam A, Akhtar S. 2018. Application of nanomaterials in civil engineering. Nanomaterials and their applications. Advanced structured materials, vol. 84. Singapore: Springer; p. 169–189.

Banfield JF, Zhang H. 2001. Nanoparticles in the environment. Rev Mineral Geochem. 44(1):1–58.

Bannunah AM, Vllasaliu D, Lord J, Stolnik S. 2014. Mechanisms of nanoparticle internalization and transport across an intestinal epithelial cell model: effect of size and surface charge. Mol Pharm. 11(12): 4363–4373.

Bayda S, Adeel M, Tuccinardi T, Cordani M, Rizzolio F. 2019. The history of nanoscience and nanotechnology: from chemical-physical applications to nanomedicine. Molecules. 25(1):112–115.

Benchimol S. 2001. p53-dependent pathways of apoptosis. Cell Death Differ. 8(11):1049–1051. www.nature.com/cdd.

Bernardeschi M, Guidi P, Scarcelli V, Frenzilli G, Nigro M. 2010. Genotoxic potential of TiO_2 on bottlenose dolphin leukocytes. Anal Bioanal Chem. 396(2):619–623.

Cedervall T, Lynch I, Foy M, Berggård T, Donnelly SC, Cagney G, Linse S, Dawson KA. 2007. Detailed identification of plasma proteins adsorbed on copolymer nanoparticles. Angew Chem Int Ed Engl. 46(30): 5754–5756.

Chen T, Yan J, Li Y. 2014. Genotoxicity of titanium dioxide nanoparticles. J Food Drug Anal. 22(1):95–104.

Clemente Z, Castro VL, Feitosa LO, Lima R, Jonsson CM, Maia AHN, Fraceto LF. 2015. Biomarker evaluation in fish after prolonged exposure to nano-TiO_2: influence of illumination conditions and crystal phase. J Nanosci Nanotechnol. 15(7):5424–5433.

Elmore S. 2007. Apoptosis: a review of programmed cell death. Toxicol Pathol. 35(4):495–516.

Falck GCM, Lindberg HK, Suhonen S, Vippola M, Vanhala E, Catalán J, Savolainen K, Norppa H. 2009. Genotoxic effects of nanosized and fine TiO_2. Hum Exp Toxicol. 28(6–7):339–352.

Fujishima A, Zhang X. 2006. Titanium dioxide photocatalysis: present situation and future approaches. CR Chim. 9(5–6):750–760.

Gholinejad Z, Khadem Ansari MH, Rasmi Y. 2019. Titanium dioxide nanoparticles induce endothelial cell apoptosis via cell membrane oxidative damage and p38, PI3K/Akt, NF-κB signaling pathways modulation. J Trace Elem Med Biol. 54:27–35.

Giovanni M, Yue J, Zhang L, Xie J, Nam C, Tai D. 2015. Pro-inflammatory responses of RAW264.7 macrophages when treated with ultralow concentrations of silver, titanium dioxide, and zinc oxide nanoparticles. J Hazard Mater. 297:146–152.

Guadagnini R, Halamoda Kenzaoui B, Walker L, Pojana G, Magdolenova Z, Bilanicova D, Saunders M, Juillerat-Jeanneret L, Marcomini A, Huk A, et al. 2015. Toxicity screenings of nanomaterials: challenges due to interference with assay processes and components of classic in vitro tests. Nanotoxicology. 9(sup1):13–24.

Gunnarsson SB, Bernfur K, Mikkelsen A, Cedervall T. 2018. Analysis of nanoparticle biomolecule complexes. Nanoscale. 10(9):4246–4257.

Hamzeh M, Sunahara GI. 2013. In vitro cytotoxicity and genotoxicity studies of titanium dioxide (TiO_2) nanoparticles in Chinese hamster lung fibroblast cells. Toxicol in vitro. 27(2):864–873.

He X, Hwang H. 2016. Nanotechnology in food science: functionality, applicability, and safety assessment. J Food Drug Anal. 24(4):671–681.

Horn BM, Schwerdtfeger CP, Meagher EP, Kristallogr Bd Z, Horn M, Schwerdtfeger CF, Meagher EP. 1972. Refinement of the structure of anatase at several temperatures. Kristallographie. 136(3–4):273–281.

Hou J, Wang L, Wang C, Zhang S, Liu H, Li S, Wang X. 2019. Toxicity and mechanisms of action of titanium dioxide nanoparticles in living organisms. J Environ Sci. 75:40–53.

Hu H, Fan X, Yin Y, Guo Q, Yang D, Wei X, Zhang B, Liu J, Wu Q, Oh Y, et al. 2019. Mechanisms of titanium dioxide nanoparticle-induced oxidative stress and modulation of plasma glucose in mice. Environ Toxicol. 34(11):1221–1235.

Hu H, Guo Q, Wang C, Ma X, He H, Oh Y, Feng Y, Wu Q, Gu N. 2015. Titanium dioxide nanoparticles increase plasma glucose via reactive oxygen species-induced insulin resistance in mice. J Appl Toxicol. 35(10):1122–1132.

Hulla JE, Sahu SC, Hayes AW. 2015. Nanotechnology: history and future. Hum Exp Toxicol. 34(12):1318–1321.

Jaeger A, Weiss DG, Jonas L, Kriehuber R. 2012. Oxidative stress-induced cytotoxic and genotoxic effects of nano-sized titanium dioxide particles in human HaCaT keratinocytes. Toxicology. 296(1–3):27–36.

Jin C, Zhu B, Wang X, Lu Q. 2008. Cytotoxicity of titanium dioxide nanoparticles in mouse fibroblast cells. Chem Res Toxicol. 21(9):1871–1877.

Kamat P. 2002. Photophysical, photochemical and photocatalytic aspects of metal nanoparticles. J Phys Chem B. 106(32):7729–7744.

Kansara K, Patel P, Shah D, Shukla RK, Singh S, Kumar A, Dhawan A. 2015. TiO_2 nanoparticles induce DNA double strand breaks and cell cycle arrest in human alveolar cells. Environ Mol Mutagen. 56(2): 204–217.

Khalil M, Jan BM, Tong CW, Berawi MA. 2017. Advanced nanomaterials in oil and gas industry: design, application and challenges. Appl Energy. 191:287–310.

Kim KT, Klaine SJ, Cho J, Kim SH, Kim SD. 2010. Oxidative stress responses of *Daphnia magna* exposed to $TiO(_2)$ nanoparticles according to size fraction. Sci Total Environ. 408(10):2268–2272.

Klingberg H, Oddershede LB, Loeschner K, Larsen EH, Loft S, Møller P. 2015. Uptake of gold nanoparticles in primary human endothelial cells. Toxicol Res. 4(3):655–666.

Kobayashi H, Sugiyama C, Morikawa Y, Hayashi M, Sofuni T. 1995. A comparison between manual microscopic analysis and computerized image analysis in the single cell gel electrophoresis assay. MMS Commun. 3(1):103–115.

Kocbek P, Teskač K, Kreft ME, Kristl J. 2010. Toxicological aspects of long-term treatment of keratinocytes with ZnO and TiO_2 nanoparticles. Small. 6(17):1908–1917.

Linkov I, Satterstrom FK, Corey LM. 2008. Nanotoxicology and nanomedicine: making hard decisions. Nanomedicine. 4(2):167–171.

Líšková A, Letašiová S, Jantová S, Brezová V, Kandarova H. 2020. Evaluation of phototoxic and cytotoxic potential of TiO_2 nanosheets in a 3D reconstructed human skin model. Altex. 37(3):441–450.

Liu N, Tang M. 2020. Toxic effects and involved molecular pathways of nanoparticles on cells and subcellular organelles. J Appl Toxicol. 40(1):16–36.

Liu N, Tang M, Ding J. 2020. Chemosphere: the interaction between nanoparticles-protein corona complex and cells and its toxic effect on cells. Chemosphere. 245:125624.

Márquez-Ramírez SG, Delgado-Buenrostro NL, Chirino YI, Iglesias GG, López-Marure R. 2012. Titanium dioxide nanoparticles inhibit proliferation and induce morphological changes and apoptosis in glial cells. Toxicology. 302(2–3):146–156.

Mosmann T. 1983. Rapid colorimetric assay for cellular growth and survival: application to proliferation and cytotoxicity assays. J Immunol Methods. 65(1–2):55–63.

Nel A, Xia T, Madler L, Li N. 2006. Toxic potential of materials at the nanolevel. Science. 311(5761):622–627.

Nel AE, Mädler L, Velegol D, Xia T, Hoek E. v, Somasundaran P, Klaessig F, Castranova V, Thompson M. 2009. Understanding biophysicochemical interactions at the nano-bio interface. Nat Mater. 8(7):543–557.

Pandey RK, Prajapati VK. 2018. Molecular and immunological toxic effects of nanoparticles. Int J Biol Macromol. 107(Pt A):1278–1293.

Park EJ, Yi J, Chung KH, Ryu DY, Choi J, Park K. 2008. Oxidative stress and apoptosis induced by titanium dioxide nanoparticles in cultured BEAS-2B cells. Toxicol Lett. 180(3):222–229.

Parkin IP, Palgrave RG. 2005. Self-cleaning coatings. J Mater Chem. 15(17):1689–1695.

Rivera-Gil P, Jimenez de Aberasturi D, Wulf V, Pelaz B, del Pino P, Zhao Y, de la Fuente JM, Ruiz de Larramendi I, Rojo T, Liang X-J, et al. 2013. The challenge to relate the physicochemical properties of colloidal nanoparticles to their cytotoxicity. Acc Chem Res. 46(3): 743–749.

Rosłon M, Jastrzębska A, Sitarz K, Książek I, Koronkiewicz M, Anuszewska E, Jaworska M, Dudkiewicz-Wilczyńska J, Ziemkowska W, Basiak D, et al. 2019. The toxicity in vitro of titanium dioxide nanoparticles modified with noble metals on mammalian cells. Int J Appl Ceram Technol. 16(2):481–493.

Samat MH, Ali AMM, Taib MFM, Hassan OH, Yahya MZA. 2016. Results in physics hubbard U calculations on optical properties of 3 d transition metal oxide. Results Phys. 6:891–896.

Sayes CM, Wahi R, Kurian PA, Liu Y, West JL, Ausman KD, Warheit DB, Colvin VL. 2006. Correlating nanoscale titania structure with toxicity: a cytotoxicity and inflammatory response study with human dermal fibroblasts and human lung epithelial cells. Toxicol Sci. 92(1):174–185.

Schindelin J, Arganda-Carreras I, Frise E, Kaynig V, Longair M, Pietzsch T, Preibisch S, Rueden C, Saalfeld S, Schmid B, et al. 2012. Fiji: an open-source platform for biological-image analysis. Nat Methods. 9(7): 676–682.

Shi H, Magaye R, Castranova V, Zhao J. 2013. Titanium dioxide nanoparticles: a review of current toxicological data. Part Fibre Toxicol. 10(1): 15.

Shukla RK, Sharma V, Pandey AK, Singh S, Sultana S, Dhawan A. 2011. Toxicology in vitro ROS-mediated genotoxicity induced by titanium dioxide nanoparticles in human epidermal cells. Toxicol in vitro. 25(1): 231–241.

Song B, Zhou T, Yang WL, Liu J, Shao LQ. 2016. Contribution of oxidative stress to TiO_2 nanoparticle-induced toxicity. Environ Toxicol Pharmacol. 48:130–140.

Stoccoro A, di Bucchianico S, Uboldi C, Coppedè F, Ponti J, Placidi C, Blosi M, Ortelli S, Costa AL, Migliore L. 2016. A panel of in vitro tests to evaluate genotoxic and morphological neoplastic transformation potential on Balb/3T3 cells by pristine and remediated titania and zirconia nanoparticles. Mutagenesis. 31(5):511–529.

Tripathi VK, Sivakumar AS, Dhasmana A, Hwang I. 2018. Crosstalk between co-cultured 3T3-L1 and C2C12 cells after the exposure of nano-titanium dioxide. J Nanosci Nanotechnol. 18(6): 3870–3879.

Vance ME, Kuiken T, Vejerano EP, McGinnis SP, Hochella MF, Rejeski D, Hull MS. 2015. Nanotechnology in the real world: redeveloping the nanomaterial consumer products inventory. Beilstein J Nanotechnol. 6(1):1769–1780.

Vroman L. 1962. Effect of absorbed proteins on the wettability of hydrophilic and hydrophobic solids. Nature. 196:476–477.

Wang J. 2001. DNA damage and apoptosis. Cell Death Differ. 8(11): 1047–1048. www.nature.com/cdd.

Weir A, Westerhoff P, Fabricius L, Hristovski K, von Goetz N. 2012. Titanium dioxide nanoparticles in food and personal care products. Environ Sci Technol. 46(4):2242–2250.

Wong-Ekkabut J, Xu Z, Triampo W, Tang IM, Tieleman DP, Monticelli L. 2007. Effect of lipid peroxidation on the properties of lipid bilayers: a molecular dynamics study. Biophys J. 93(12):4225–4236.

Wu X, Tan Y, Mao H, Zhang M. 2010. Toxic effects of iron oxide nanoparticles on human umbilical vein endothelial cells. Int J Nanomedicine. 5:385–99.